

The Spall Strength and Hugoniot Elastic Limit of Tantalum with Various Grain Size

S.V.Razorenov¹, G.V.Garkushin¹, G.I.Kanel¹, O.N.Ignatova²

¹ Institute of Problems of Chemical Physics RAS, Chernogolovka, Moscow region, 142432 Russia

² Russian Federal Nuclear Center, VNIIEF, Sarov, Nizhni Novgorod region 607190 Russia

razsv@ficp.ac.ru garkushin@ficp.ac.ru kanel@ficp.ac.ru o.n.ignatova@gmail.com

Keywords: Shock wave, tantalum, spall fracture, HEL, ultra fine grained structure.

Abstract. The VISAR free surface velocity histories have been measured for commercial grade coarse grain (CG, 50 – 60 μm) and ultra fine grained (UFG, ~ 0.5 μm grain size) after severe plastic deformation tantalum and for comparison tantalum single crystals, at peak stresses around 12-14 GPa and strain rates of 10^5 – 10^6 s^{-1} . The decrease in the grain size, which resulted in ~ 25 % increase of the hardness did not cause any significant influence on the HEL, the value of which is ~ 2 GPa, but increases slightly the spall strength of the UFG tantalum (7.4 GPa) in comparison with the CG samples (~ 7 GPa). In both cases the spall strength does not noticeably vary with increase of the peak shock stress up to 70 GPa. The experiments using samples precompressed at 40 and 100 GPa peak pressure have confirmed weak influence of preceding shock compression on the tantalum spall strength. The tantalum single crystals display the highest spall strength equal to ~ 10 GPa. The influences of the grain size on static and dynamic yield stresses are discussed in terms of general strain rate effects.

Introduction

It is well known that dynamic deformation leads to hardening of metals and alloys due to storage of defects [1] and reduction of grain sizes under severe plastic deformation [2]. On the other hand, the data on the influence of these factors on flow stresses and material strength under high strain rates is very sparse and often contradictory [3,4].

The interest in the dynamic strength of tantalum is connected with its industrial applications under strong impulse stresses. Tantalum has a high density (16.65 g/cm^3), melting temperature (2996 $^{\circ}\text{C}$) and is unique in its combination of high hardness with high plasticity. Extensive research and publications are dedicated to investigations of the elastic-plastic properties and spall fracture of tantalum under shock-wave loading [5-9], but the question about the influence of structural factors on these processes remains unanswered.

In this work, the VISAR free surface velocity histories have been measured for commercial grade tantalum with various grain sizes and structural defects, and for comparison, tantalum single crystals to get information about the elastic-plastic transition and the resistance to spall fracture.

Material and experiment

The tantalum samples in as-received state (CG) had an average grain size ~ 50 - 60 μm . The ultra-fine grain structure (UFG) was obtained by forging in three directions at decreasing temperature starting from 800 $^{\circ}\text{C}$. As a result of severe plastic deformation, a uniform structure was achieved with an average grain size ~ 0.5 – 0.7 μm . The microstructure of CG and UFG tantalum samples are presented in Figure 1. It is seen from these pictures, that the deformed samples have rather uniform structure without strongly marked zones of different granularity. However, as the electron microscopy displays, the structure contains less than 1 % of larger extended grains with the size up to 4 μm . After the three-dimensional forging the twins in the grain structure of tantalum are not observed.

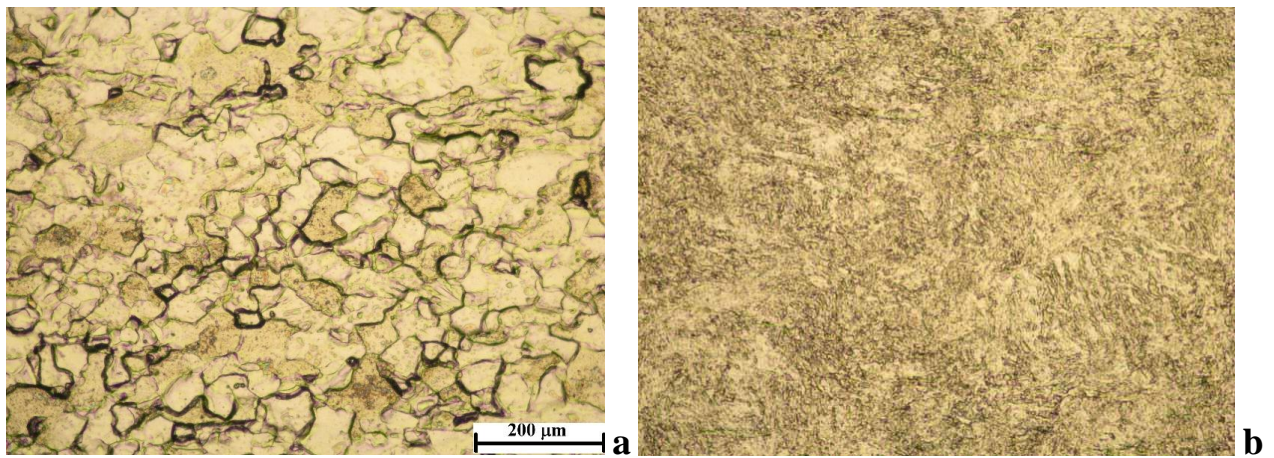


Fig.1. Microstructures of as-received (a) and ultra fine grain (b) tantalum tested.

The unsoundness of CG and UFG tantalum samples was varied by means of shock wave of ~40 and ~100 GPa intensity. Figure 2 presents the photograph of microstructure of as-received tantalum sample recovered after shock loading of ~25 GPa intensity.

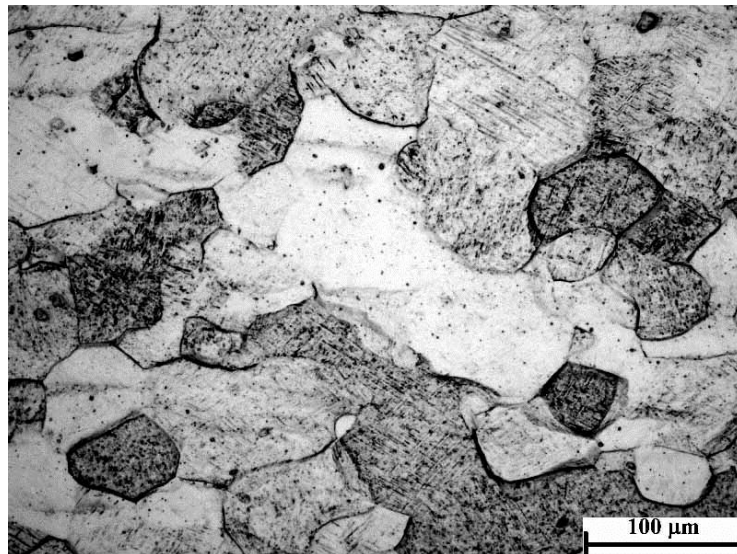


Fig.2. Microstructure of as-received tantalum sample subjected by shock wave loading of 25 GPa amplitude.

As it can see from this figure, the forming of the bands of local deformations (twins) is observed practically in all grains. Metallography of recovered preshock samples has shown up the twin structure of 10-20% concentration at 40 – 60 GPa, which decreased under pressure growth due to the annealing of material with increasing of shock temperature. In UFG samples, the concentration of twins was found close to zero. Dislocation density increased from $0.5 \times 10^{10} \text{ cm}^{-2}$ to $2 \times 10^{10} \text{ cm}^{-2}$ at 100 GPa. A few experiments were done with tantalum single crystals of uncertain orientation.

The data about hardness measured for all tantalum samples tested are presented in Table 1. From Table it is clear, that both severe static plastic deformation and preshock deformation increase hardness of CG samples by ~25%, but the preshock deformation did not change the hardness of UFG samples.

Table 1. The hardness of tantalum in various structural states.

Sample	Hardness, HRB
As-received (CG) (grain size $\sim 55 \mu\text{m}$)	76 – 79
Ultra-fine grained (UFG) ($\sim 0.5 \mu\text{m}$)	103 – 104
Shock precompressed CG ($\sim 40 \text{ GPa}$)	103
Shock precompressed CG ($\sim 100 \text{ GPa}$)	97 – 99
Shock precompressed UFG ($\sim 40 \text{ GPa}$)	104 – 105
Shock precompressed UFG ($\sim 100 \text{ GPa}$)	103 – 105
Single crystal	68

The experiments were carried out with the tantalum samples of $\sim 0.6 \text{ mm}$ or $\sim 2 \text{ mm}$ in thickness and linear sizes of $25 - 30 \text{ mm}$. The shock compression pulses were generated with the impact of an aluminum plates of ~ 0.1 or 0.4 mm in thickness, which were accelerated up to 1250 m/s with an explosive device [10]. Experiments with the samples of different thickness enabled us to change the strain rate of the tantalum samples before fracture in rarefaction wave with the factor of five. In all experiments, the free surface velocity histories $u_{fs}(t)$ were measured using a VISAR velocimeter [11] with a time resolution of $\sim 1 \text{ ns}$.

Results and Discussion

In Fig.3, the results of free surface velocity profile measurements $u_{fs}(t)$ for as-received (CG) and ultra-fine grained (UFG) tantalum are compared. All profiles are typical for those obtained for other metals under spall conditions [10]. These profiles demonstrate significant decay of elastic precursors with the distance both for CG and UFG tantalum samples tested. This decay is induced by deviator stress relaxation due to development of plastic deformation directly behind of elastic wave. The compressive stress behind the front of the elastic precursor – the Hugoniot Elastic Limit is calculated as $\sigma_{HEL} = 1/2 \rho_0 c_l u_{HEL}$. Yield strength is determined from the HEL as $Y = 3/2 \sigma_{HEL} (1 - c_b^2 / c_l^2)$, where ρ_0 – material density, c_b , c_l – bulk and longitudinal sound speeds, u_{HEL} – elastic precursor amplitude.

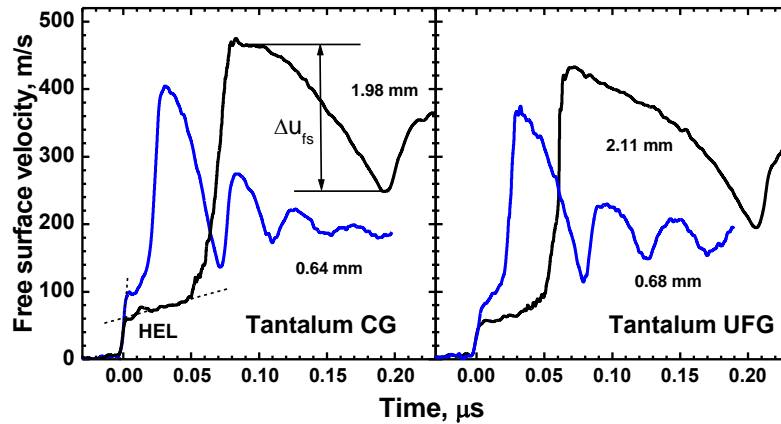


Fig. 3. Free-surface velocity profiles of CG and UFG tantalum samples of different thicknesses.

The decrease of the HEL in CG samples with the distance was from 3.24 GPa at 0.64 mm of sample thickness to 2.12 GPa at 1.98 mm , and from 2.66 GPa at 0.68 mm to 1.83 GPa at 2.11 mm

for UFG samples. The reduction of grain sizes after SPD processing resulted in decreasing of UFG tantalum elastic limit, when the hardness of UFG samples is higher by ~25% (Table 1).

As it can be seen from the profiles in Fig.1, the rise time of parameters in plastic shock wave is noticeably less for UFG samples, than for CG tantalum. It indicates the higher plastic strain rates and less characteristic viscosity $\tau/\dot{\epsilon}$ of tantalum. Maximum compression rates and accompanying maximum acceleration of sample surfaces in plastic shock front measured were estimated equal to $3.5 \times 10^6 \text{s}^{-1}$ for CG and $6.4 \times 10^6 \text{s}^{-1}$ for UFG tantalum samples. Perhaps, the observed difference of grain size reducing effect under low strain rate conditions and under shock-wave compression is explained by different stress relaxation rates in CG and UFG tantalum samples, as shown in Fig.4.

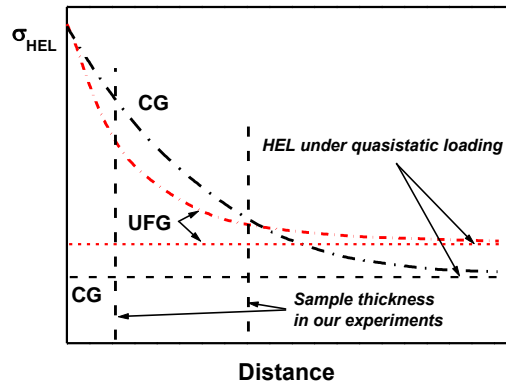


Fig. 4. The assumed difference of decay rates of elastic precursors in CG and UFG tantalum.

At long distances, the Hugoniot elastic limit has to approach to the values of HEL under quasistatic loading conditions. It means, the HEL of thick UFG samples (more than 2 mm for our case) must be higher than the elastic limit of CG thick samples. However, since characteristic viscosity of UFG samples is less, than CG samples, the decay of elastic precursor occurs faster. As result, a situation is possible, when harder UFG tantalum demonstrates lower values of HEL for thin samples (less of ~2 mm), than CG tantalum.

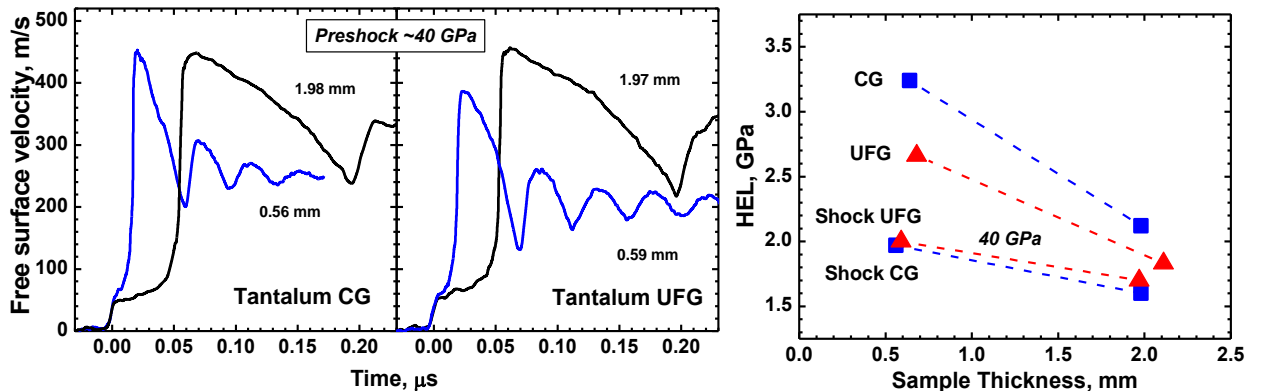


Fig. 5. Free-surface velocity profiles of CG and UFG tantalum samples of different thicknesses after previous shock wave deformation.

Fig. 6. The decay of elastic precursors in CG, UFG and preshocked at 40 GPa tantalum samples.

The results of experiments with CG and UFG tantalum samples, previously exposed to shock-wave loading of intensity ~40 GPa, are presented in Fig.5. In Fig.6, the results of Hugoniot elastic limit measurements for all types of tantalum samples of different thicknesses are summarized. The previous shock deformation leads to decreasing of HEL and decay rates of elastic precursors both

for CG and UFG tantalum. The compression rate of the plastic shock wave increased after preshock processing up to $(0.95-1.1)\times 10^7 \text{ s}^{-1}$ and differentiates little between CG and UFG samples.

The decreasing of HEL due to preshock deformation is much higher for CG samples than for UFG ones; and as the result the difference of HEL for CG and UFG tantalum becomes very little. Increasing the intensity of previous shock deformation up to 100 GPa does not change the parameters of elastic-plastic transition, increasing the dispersion of elastic wave front only.

The spall strength of all types of tantalum samples tested σ_{sp} was calculated from the analysis of wave profiles [10] using measured “velocity pullback” (Δu_{fs}) as $\sigma_{sp} = 1/2\rho_0 c_b(\Delta u_{fs} + \delta u)$, where ρ_0 is the density of a material, δu is the correction for the distortion of the waveform due to a difference between the velocity (c_l) of the spall pulse front propagation over the stretched material and the velocity (c_b) of the plastic portion of the incident unloading wave ahead of it. Here c_l and c_b are the longitudinal and bulk sound speeds, correspondingly.

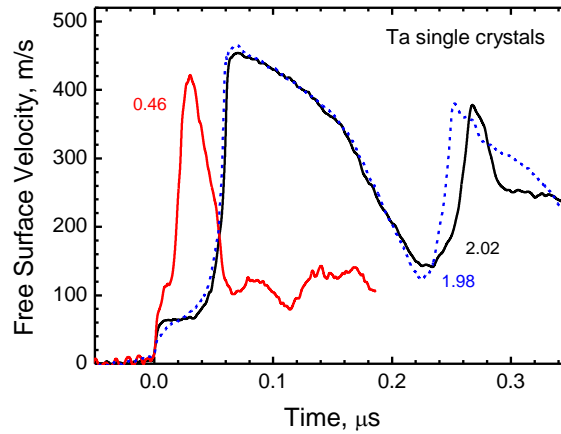


Fig.7. The results of measurements of free surface velocity profiles of samples of tantalum single crystals. The sample thicknesses are shown alongside the waveforms in millimeters.

The measurements of spall strength of tantalum with different grain structure were supplemented with experiments on the tantalum single crystals. The single crystals orientation concerning the direction of shock loading propagation was not defined. In Fig.7 the wave profiles obtained in these experiments are represented. As it was expected, the tantalum single crystals have the highest spall strength. Directly from the comparison of waveforms in Fig 3,5 and 7 it is clear that, the single crystals free of structural defects demonstrate much higher resistance to the spall fracture, than the polycrystalline tantalum, what is connected with the absent of coarse defects of microstructure as the sites of spall fracture nucleation. At this, according to the form of the wave profile of thin sample of single crystal (Fig.7), it is seen that at the moment before the spall pulse, the strength resource of the material in this experiment is not completely realized and, probably, the higher values of the spall strength could be registered under the higher peak pressure of shock compression.

The measurement results are summarized in Table 2 and Figure 8 in the form of a dependence of the tantalum spall strength on the strain rate in the unloading part of the shock pulse, calculated as $\dot{V}/V_0 = -\dot{u}_{fsr}/2c_b$, where \dot{u}_{fsr} is the measured free-surface velocity gradient in the unloading portion of the incident compression pulse.

One can see that the decrease of the grain size has led to a ~5% increase of the spall strength of tantalum. This effect is a little higher under longer impulse of shock loading. The previous shock-wave deformation of both sample types (CG and UFG) had a negligible influence on the value of the fracture stresses. Similar effect was observed in spall experiments with the fivefold increase of shock loading intensity, when impactor velocity was ~4100 m/s and, as result, the peak pressure in

this case was more ~70 GPa. Perhaps, the twins and dislocation, in shock wave generated, influence weakly the character of spall fracture nucleation in tantalum over this strain rate range.

Table 2. Experimental data on strength properties of Tantalum with various grain sizes.

Shot #	$h_{sam.}, [mm]$	$h_{imp.}, [mm]$	$\sigma_{HEL}, [GPa]$	$Y, [GPa]$	$\sigma_{sp.}, [GPa]$	$h_{sp.}, [mm]$	$\dot{v}/v_0, [10^5 s^{-1}]$
Tantalum as-received (CG)							
#20	1.97	0.4	2.12	1.02	6.7	0.21	3.1
#21	0.64	0.11	3.24	1.56	8.1	0.08	13
Tantalum ultra-fine grained (UFG)							
#9	2.14	0.41	2.05	0.99	7.1	0.26	4.5
#10	2.11	0.41	1.83	0.88	7.6	0.26	4.8
#11	0.68	0.12	2.66	1.28	7.9	0.09	12
#12	0.54	0.12	2.2	1.06	8.4	0.07	19
Tantalum (CG) shock precompressed, 40 GPa							
#18	1.97	0.41	1.6	0.77	6.5	0.24	3.7
#19	0.56	0.11	1.97	0.95	7.6	0.08	12
Tantalum (UFG) shock precompressed, 40 GPa							
#22	1.97	0.41	1.7	0.82	7.5	0.25	4.7
#23	0.59	0.11	2.0	0.96	7.9	0.09	14
Tantalum shock precompressed, 100 GPa							
#25(CG)	1.92	0.41	1.5	0.72	6.9	0.29	3
#24(UFG)	1.97	0.41	—	—	7.4	0.25	3.9
Tantalum (CG), impact velocity 4.1 km/s							
#27	1.98	0.38	—	—	7.3	0.084	8.5
Tantalum single crystal							
#13	2.02	0.41	2.2	1.06	9.4	0.3	3.9
#15	1.98	0.41	1.7	0.82	10.4	0.29	5
#16	0.46	0.12	—	—	9.6	0.09	6

The results of this work together with the data of French authors on tantalum spall strength over a wide range of strain rates are presented in Figure 9 [6,8].

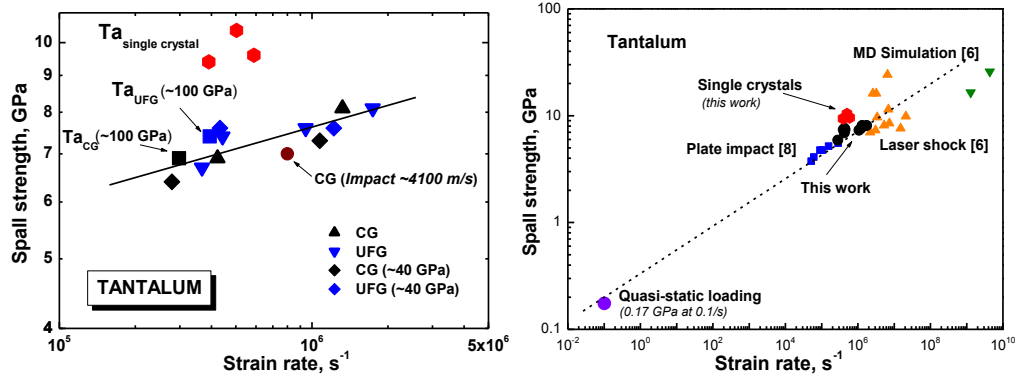


Fig. 8. Spall strength of tantalum in various structural states.

Fig. 9. The dependence of tantalum spall strength on strain rates of different authors from the quasi-static loading conditions to picosecond load duration.

Our data is in good agreement with the data under dynamic loading, and general dependence is reasonable extrapolated to tantalum strength value under quasi-static loading. One can see that unlike plate impact experiments, under short laser pulse loading the data spread in spall strength can reach 50%. Perhaps, this occurs in experiments with very thin samples, when the spall plate thicknesses are less, than the grain sizes.

Conclusion

Thus, the new data about strength properties of high purity commercial Ta with various grain structure under the condition of shock-wave loading in submicrosecond range of the load durations are obtained. The most interesting and unexpected result was that the decreasing of the grain size from 60 μm to 1 μm by severe plastic deformation, which led to growth of the material hardness approximately by 25%, gave the reverse effect on the value of the yield strength of tantalum. The effect is explained by the high rate of stress relaxation in fine grained material. The fast stress relaxation in fine grain material becomes apparent under the higher rates of compression in the plastic shock wave. Evidently, the grain boundaries are the sites of dislocation nucleation under these conditions, which provide higher rate of deformation in the fine grain material.

The hardening of tantalum by shock wave with the pressure of 40-100 GPa also led to the growth of stress relaxation rate, decrease of yield strength and disappearing of the difference of its values for coarse grained and fine grained materials. The measurements conducted didn't reveal the noticeable influence of the severe static plastic deformation, so as strong deformation of tantalum at the shock compression on its strength characteristics under the conditions of spall fracture. The decreasing of grain size as a result of the previous severe plastic deformation leads to insignificant growth of spall strength (approximately by 5%) and decreasing of dynamic viscosity of tantalum, but the Hugoniot elastic limit and the character of elastic-plastic transition practically do not depend on the grain size. Previous shock compression of as-received samples up to 40 GPa leads to insignificant (~14%) decreasing of the spall strength and dynamic viscosity of tantalum, but does not influence the character of the elastic-plastic transition and the value of the Hugoniot elastic limit. The change of inner structure as a result of previous shock compression up to ~100 GPa leads to decreasing of the elastic limit of tantalum approximately by 30%. Strength behavior of submicrocrystalline samples, recovered after the previous shock pressure with intensity of ~40 and 100 GPa, practically does not differ from the behavior of as-received tantalum.

The quintuple increasing of the shock compression pressure, preceding to the spall fracture, also did not lead to a noticeable change of the fracture stress value. Apparently, twins and dislocations, generated by shock wave, can make a small contribution in the damage nucleation, at least, in the investigated range of strain rates.

Maximum fracture stresses are realized in the samples of single crystal tantalum. Increasing of the strain rate under tension results in the growth of fracture stresses in tantalum, irrespective of its inner structure. In addition, the conducted experiments with tantalum of different structures confirm the existence of correlation between the influence on the strength properties of metals and alloys by severe dynamic and static deformation, in spite of the difference in their mechanisms.

Acknowledgements

This work was supported by the Russian Foundation for Basic Research, Grant № 08-02-00087a, and The State Atomic Energy Corporation ROSATOM, Grant № H.4e.45.03.09.1073. The authors thank Prof. Salischev G.A. for the help in preparing and testing of tantalum samples microstructure and Ermolov L.G. for the help in explosive experiments.

References

- [1]. Meyers M.A., Murr L.E. "Shock waves and high-strain-rate phenomena in metals". 1984, Plenum Press. NY and London.
- [2]. Valiev R.Z., Alexandrov I.V. "Bulk nanostructural metal material: production, structure and properties." 2007, Academkniga, Moscow, 398 p.
- [3]. Garkushin G.V., Ignatova O.N., Kanel G.I., Meyer L., Razorenov S.V. Mech. of Solids, N.4, p.155, 2010.
- [4]. Razorenov S.V., Garkushin G.V., Kanel'G.I., et al. Phys.Solid State, **53**, N.4, pp. 824–829, 2011.
- [5]. Furnish M.D., Reinhart W.D., Trott W.M., et al. In: Shock compression in condensed matter - 2005, Ed.: Furnish M.D., et.al., 2006, AIP Conf. Proc., p.p.615.
- [6]. Cuq-Lelandias J.P., Boustie M., Soulard L., et.al.. RPJ Web of Conferences, **10**, 00014, 2010.
- [7]. Asay J.R., Ao T., Vogler T.J., Davis J.-P., Gray III G.T. J. Appl. Phys., **106**, 073515, 2009.
- [8]. Roy G.. Thesis of doc. of sci., Univ. of Poitiers, 2003.
- [9]. Bingert J.F., Henrie B.L., Worthington D.L. Metallurgical and Materials Transformations A, **38A**, p.1712, 2007.
- [10]. Antoun T., Seaman L., Curran D.R. , Kanel G.I., Razorenov S.V., Utkin A.V. "Spall Fracture." 2003, Springer, New York, 404 p.
- [11]. Barker L.M., and Hollenback R.E., J.App. Phys. **43**, p. 4669, 1972.